

Supplementary Information:

Computational design of antimicrobial active surfaces via automated Bayesian optimization

Hanfeng Zhai and Jingjie Yeo*

Sibley School of Mechanical and Aerospace Engineering,

Cornell University, Ithaca, NY 14850, USA

E-mail: jingjieyeo@cornell.edu

1 Geometric Extraction

To finalize the geometric design corresponding to each scenarios, all the extracted data are visualized in Figures S1, S2, S3, S4. For each figure, the data representation of radii R_x to R_y , height h , and cone numbers per box side n , are shown in sub-figures A, B, and C, respectively. Note that different n values are marked in different colors. We do so because each n represents a totally different geometric design as n is an integer and should not be averaged over the extracted designs. Hence, we select the n value to repeat the most times among the extracted designs and averaged the corresponding R_x , R_y , and h for representative geometries selection, marked in red in sub-figures A and B. The box plot for visualizing the data distribution of the diameters and heights is shown in the sub-figures D, E, and F, respectively. Note that the mean value is marked in each sub-figure.

Based on the mean values of the radii and heights corresponding to the most frequent cone numbers, the extracted optimized geometries for the four different scenarios are shown

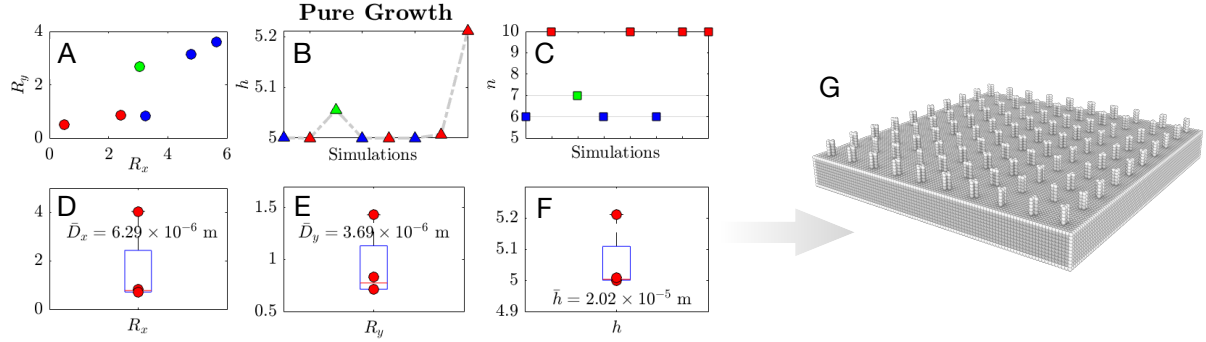


FIGURE S1: The process for geometry selection for resisting pure biofilm growth. (A) The upper and lower radii R_x to R_y diagram. (B) The heights of the extracted geometries along the simulations. (C) The cone numbers per box side of the extracted geometries along the simulations. (D) The boxplot for upper diameter D_x of the extracted geometries, where \bar{D}_x is the mean value. (E) The boxplot for lower diameter D_y of the extracted geometries, where \bar{D}_y is the mean value. (F) The boxplot for height h of the extracted geometries, where \bar{h} is the mean value. (G) Visualization of the extracted geometry.

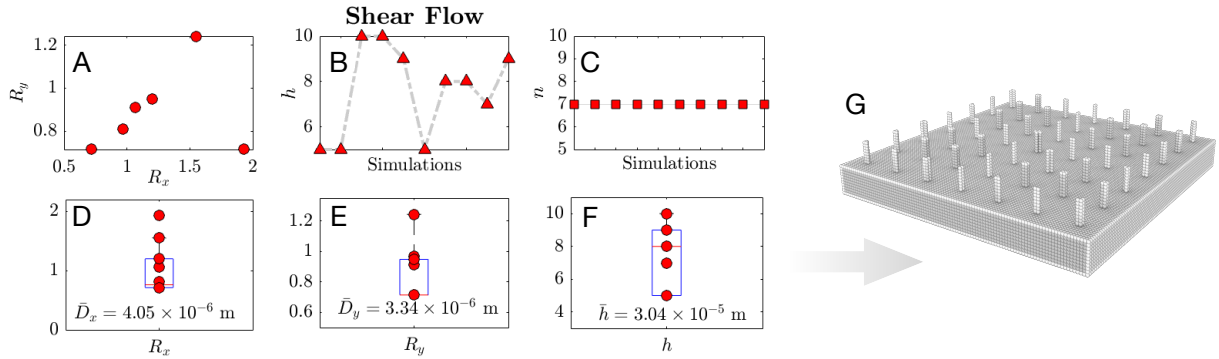


FIGURE S2: The process for geometry selection for shear flow biofilm removal. (A) The upper and lower radii R_x to R_y diagram. (B) The heights of the extracted geometries along the simulations. (C) The cone numbers per box side of the extracted geometries along the simulations. (D) The boxplot for upper diameter D_x of the extracted geometries, where \bar{D}_x is the mean value. (E) The boxplot for lower diameter D_y of the extracted geometries, where \bar{D}_y is the mean value. (F) The boxplot for height h of the extracted geometries, where \bar{h} is the mean value. (G) Visualization of the extracted geometry.

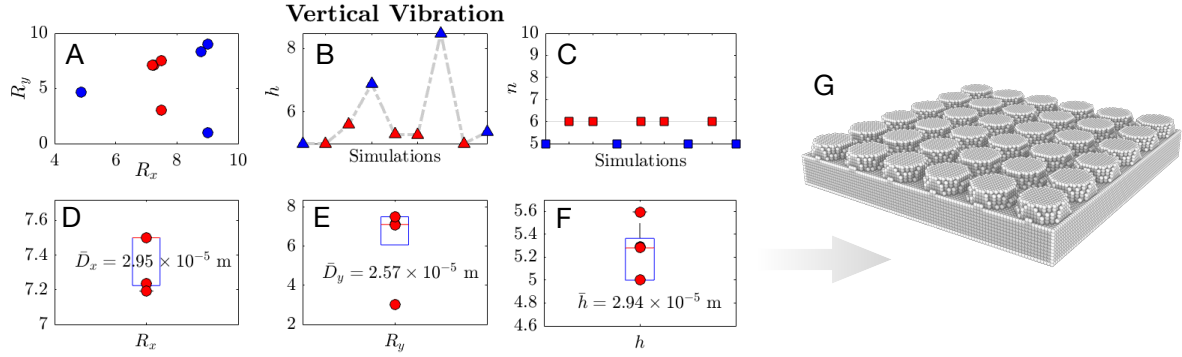


FIGURE S3: The process for geometry selection for vertical vibrational biofilm removal. (A) The upper and lower radii R_x to R_y diagram. (B) The heights of the extracted geometries along the simulations. (C) The cone numbers per box side of the extracted geometries along the simulations. (D) The boxplot for upper diameter D_x of the extracted geometries, where \bar{D}_x is the mean value. (E) The boxplot for lower diameter D_y of the extracted geometries, where \bar{D}_y is the mean value. (F) The boxplot for height h of the extracted geometries, where \bar{h} is the mean value. (G) Visualization of the extracted geometry.

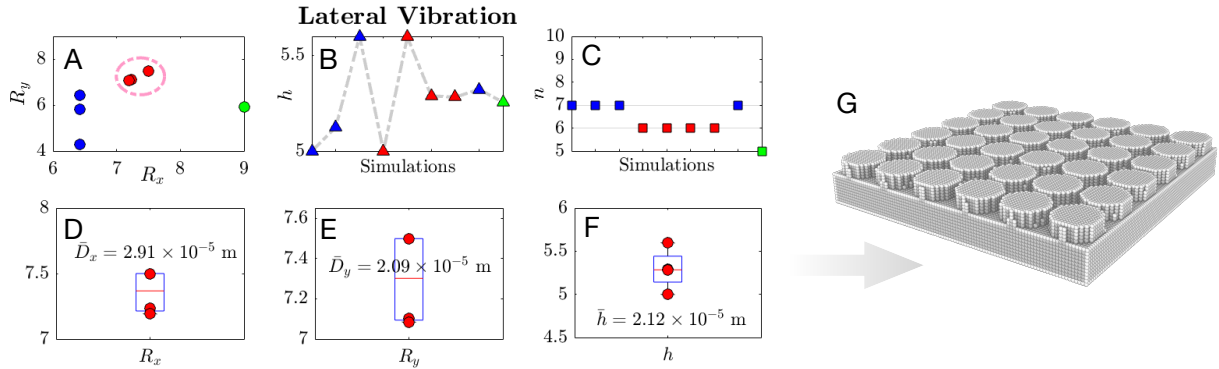


FIGURE S4: The process for geometry selection for lateral vibrational biofilm growth. (A) The upper and lower radii R_x to R_y diagram. (B) The heights of the extracted geometries along the simulations. (C) The cone numbers per box side of the extracted geometries along the simulations. (D) The boxplot for upper diameter D_x of the extracted geometries, where \bar{D}_x is the mean value. (E) The boxplot for lower diameter D_y of the extracted geometries, where \bar{D}_y is the mean value. (F) The boxplot for height h of the extracted geometries, where \bar{h} is the mean value. (G) Visualization of the extracted geometry.

in sub-figure G, and the corresponding parameters are tabulated in the main article. The four optimized geometries display exceedingly different characteristics: to purely minimize biofilm formation, the optimal geometry is 10×10 cones with relatively small radii and low height. To efficiently remove biofilm under shear flow, the optimal geometry is taller cones with small radii and a larger distance between cones with cone numbers of 7×7 . For both cases of applied vertical and lateral vibration, the optimized geometries have similar characteristics: total cones of 6×6 with short and thick cones.

2 Illustration for Biofilm Adhesion

Figure S5 visualizes the process to extract bacteria number distribution along the Z axis. We first output all the height information of the bacteria cells marked in blue. All the data are sampled as discrete points in red. The red dots are then connected through lines to represent the bacteria distribution.

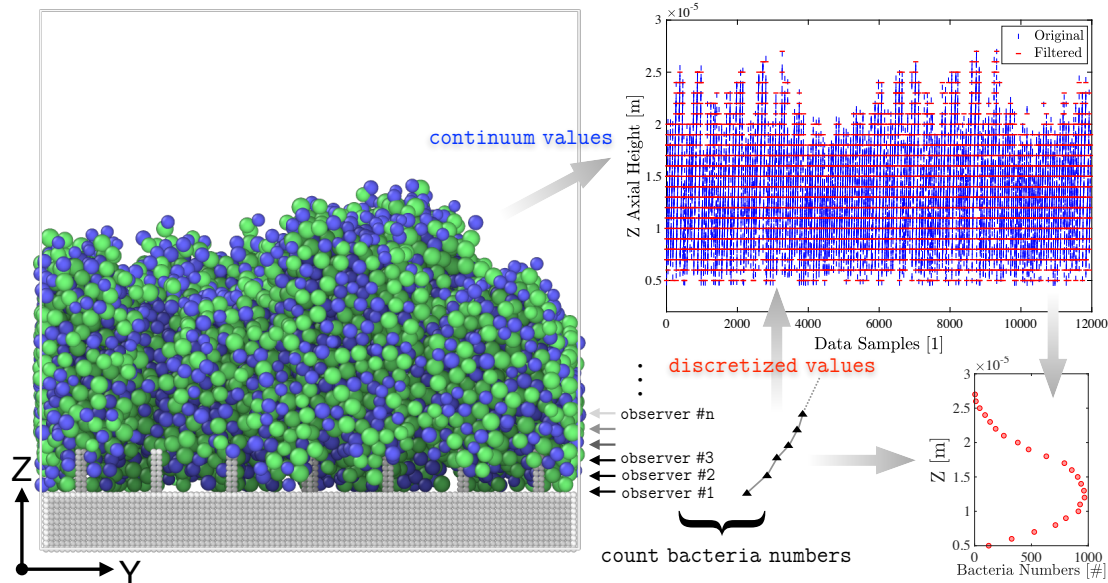


FIGURE S5: The process of counting the bacteria numbers along the Z axis. The continuous values (blue) are sampled at discrete positions (red) for visualization.

3 Technical Implementation of Automated BO

The design variables are passed from Python to LAMMPS via the mentioned Python-LAMMPS interface. The corresponding objective value obtained in the LAMMPS simulations is then passed to the BO algorithm in Python to generate a new set of design variables. The optimization loops cease at the preset iteration steps.

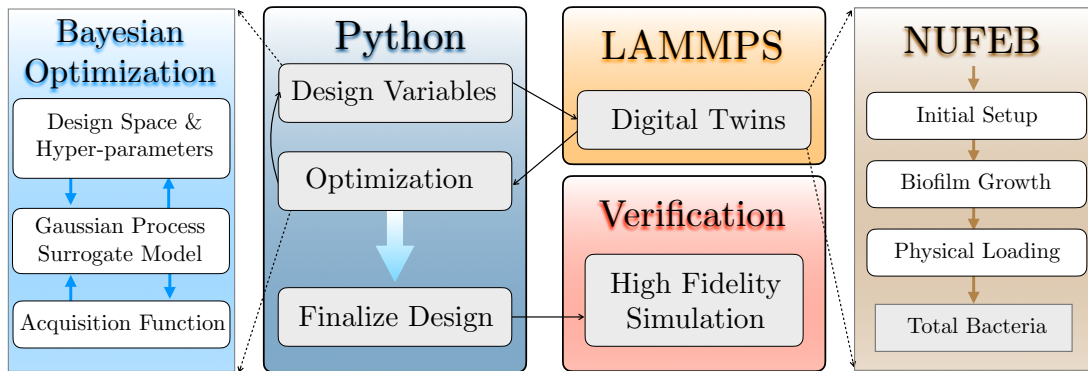


FIGURE S6: The technical implementation for the proposed automated Bayesian optimization.